Novel Three-Dimensional Electrodes: Electrochemical Properties of Carbon Nanotube Ensembles

Jun Li,*,† Alan Cassell,† Lance Delzeit, Jie Han,† and M. Meyyappan

NASA Ames Research Center, Moffett Field, California 94035

Received: May 14, 2002; In Final Form: July 11, 2002

We report on the electrochemical study of three carbon nanotube ensemble electrodes: single-walled nanotube paper, as-produced multiwalled nanotube towers, and heat-treated multiwalled nanotube towers. Cyclic voltammetry was used in 0.10 M KCl containing 5.0 mM $K_4Fe(CN)_6$ to obtain information on both the capacitive background and electron transfer rate from the faradaic reaction of the redox species. The capacitance gives insight into the effective surface area (including both the exterior surface and the interior surface within the film) as well as the "pseudocapacitance" due to faradaic reactions of surface bonded oxides. We found that a large portion of the carbon nanotube surface of the as-produced multiwalled nanotube tower electrode was blocked by amorphous carbon. It can be largely removed by prolonged heat treatment. Among the three types of samples, the single-walled nanotube paper electrode presented the largest volume specific capacitance, consistent with its highest carbon nanotube packing density (i.e., largest effective carbon nanotube surface area). The redox reaction of $Fe(CN)_6^{3-}/Fe(CN)_6^{4-}$ was found to occur not only at the outer surface of the carbon nanotube film but also at the interior surface of the nanotube ensemble electrodes. This indicates that the carbon nanotube ensemble behaves as a three-dimensional electrode. The apparent electron transfer rate (as indicated by the redox peak separation) was found to correlate to both the area of the exposed side-walls (with graphite basal-plane-like properties) and the density of graphite edge-plane-like defects.

Carbon nanotubes (CNTs) consisting of seamless cylindrical graphitic sheets, have emerged as a new class of materials with intriguing nanometer scale structures and unique properties,[1–4] which attracted intensive attention in many fields such as nanoelectronic devices, composite materials, field-emission devices, atomic force microscope probes, gas and chemical sensors, and lithium ion storage. CNTs can also be used as potential nanoscale building blocks to construct three-dimensional (3-D) nanoelectrode ensembles that are not readily available with other materials. From a chemistry point of view, CNTs are expected to exhibit inherent electrochemical properties similar to other carbon electrodes widely used in various electrochemical applications.[5] In addition, the finite size of CNTs is expected to provide added advantages demonstrated by Martin et al. with other nanoelectrode ensembles.[6] It is important to investigate fundamental electrochemical properties of CNT electrodes regarding background, capacitance, and electron transfer rate, particularly in the ensemble configuration.

In this paper, we report on the electrochemical study of three different CNT ensemble electrodes including single-walled nanotube paper (SWNTP), multiwalled nanotube towers (MWNTTs), and heat-treated multiwalled nanotube towers. The study provides systematic information to correlate electrochemical properties of different nanotube materials with their ensemble structures. It reveals that the CNT packing density in the ensemble and pretreatment are important factors defining the performance of the electrodes.

Unlike other carbon-based nanomaterials such as C_{60} and C_{70},[7] CNTs show very different electrochemical properties. Liu et al.[8] compared a single-walled carbon nanotube (SWNT) film

with that of a C_{60} film cast in the same way from suspensions on a Pt or Au electrode. The cyclic voltammetry (CV) of a SWNT film showed a broad featureless curve with a large effective capacitance in contrast to that of the C_{60} film showing several pairs of discrete redox waves. Liu et al. attributed the featureless CV and large effective capacitance to two possibilities: (1) an average of many closely spaced peaks corresponding to nanotubes with different length, diameter, and helicity, and (2) CNTs behaving like bulk carbon materials with high effective surface area rather than individual redox active molecules. Even though the exact mechanism is not clear, the high specific capacitance was proposed for the application as supercapacitors. Barisci et al.[9] further investigated the capacitance behavior of SWNTP electrodes and suggested that the large surface area and surface bonded oxides are mainly responsible for the capacitance.

While most of the initial electrochemical studies on CNTs were carried out with SWNTs due to their unique molecular structures, multiwalled carbon nanotubes (MWNTs) are potentially more attractive electrode materials. Generally, MWNTs have larger diameters and better electrical conductivity compared to SWNTs. They can be used as simple conducting wires[10] to build single nanoelectrodes, 2-D, or 3-D nanoelectrode ensembles. Chen et al. indicate that MWNT films also show large specific capacitance.[11] Other studies indicate that MWNTs have a fast electron transfer rate for various redox reactions. Campbell et al. demonstrated that a single multiwalled carbon nanotube electrode (~200 nm in dia.) presents the ideal steady-state radial diffusion feature.[12] The limiting current was found to scale linearly with the depth of immersion, consistent with a fast electron transfer between $Ru(NH_3)_6^{3+}$ and the amorphous carbon covered MWNT electrode. Ajayan et al. demonstrated the ideal

---

* Corresponding author. E-mail: jli@mail.arc.nasa.gov
† Also at Eloret Corporation.

Nernstien behavior and fast electron transfer kinetics for a redox couple $Fe(CN)_6^{3-}/Fe(CN)_6^{4-}$ with a micron sized MWNT bundle electrode.[13] It would be interesting to explore both the capacitance and electron transfer issues of MWNTs in ensembles.

We investigate here the electrochemical properties of three types of 3-D CNT ensembles: single-walled nanotube paper, as-produced multiwalled nanotube towers, and heat-treated multiwalled nanotube towers. The $Fe(CN)_6^{3-}/Fe(CN)_6^{4-}$ couple was used as a benchmark to characterize the electron transfer properties of the electrodes. We found that the ensemble electrodes present properties different from either solid macroelectrodes or single nano-/microelectrodes due to the highly porous 3-D nature. The density and surface purity of CNTs are critical for their applications.

Experimental Section

SWNTs produced by the laser ablation method[14] were obtained from NASA Johnson Space Center. The raw SWNT material was composed of $\sim$35−40% SWNTs and other impurities including graphite encapsulated catalyst particles, amorphous carbon, fullerenes, etc. Removal of the unwanted materials was accomplished by refluxing in 2.6 M HNO_3 for 45 h,[15] and the relative purity was confirmed using transmission electron microscopy. The remaining solids were spun down using ultracentrifugation (4000 g), and the solids were collected as SWNT paper on cellulose nitrate filtration membranes (0.45 μm pore size, Nalgene). It consisted of randomly but intactly stacked SWNT bundles. Each bundle (about 10 to 20 nm dia.) consisted of $\sim$100 SWNTs with a length of over 10 microns.[14,15] The paper was then rinsed with 0.01 M NaOH (pH 10) three times, and finally with water before drying in a vacuum oven overnight (60 °C). The paper spontaneously separated from the cellulose nitrate membrane, thus giving pure SWNT based paper with purity above 99%. The thickness employed in our experiments varied from about 10 μm to 100 μm. The paper was cut into a strip and sealed in a 3 mm dia. plastic tube with epoxy (Sigma-Aldrich), leaving about 3 mm × 5 mm area extending out. A copper wire was placed inside the tube and connected to the SWNT paper using silver paste.

The MWNTTs were grown by thermal CVD with ethylene feedstock at 750 °C on a piece of Si wafer which was coated with a 10 to 20 nm thick Al film (as an electrical conductive layer) followed by a 10 nm thick Fe film (as the catalyst) prepared with ion sputtering.[16] The CNT film thickness varies from 30 μm to 100 μm. Electrochemical measurements were carried out with a sample about 3 mm × 3 mm submerged into the electrolyte solution. For some experiments, the MWNTT sample was placed in a tube furnace and heated to 450 °C for about 10 h in air. The heat treatment removed most of the amorphous carbon presented in the as-produced sample and showed quite different results. A carbon paste electrode (CPE) and a glassy carbon electrode (GCE) were used for comparison. An Ag/AgCl (3M KCl) reference electrode with a frit (EG&G) and a coiled Pt (Alfa Aesar) counter electrode were employed in all electrochemical measurements. $K_4Fe(CN)_6$ (5 mM, Aldrich) dissolved in KCl (0.10 M, Aldrich) was used to characterize the CNT electrodes. All electrochemical measurements were carried out with an Autolab system (Autolab with PGSTAT12, Eco Chemie B. V.).

CNT electrodes, particularly those never used before for electrochemical experiments, were often found to contain a thin air film at the surface when submerged into the aqueous electrolyte solution. This is due to the high hydrophobicity of
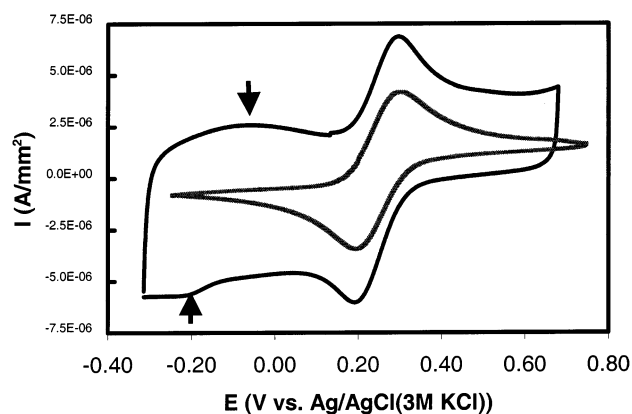

Figure 1. Cyclic voltammetry obtained with a SWNTP (outer lines) and carbon paste electrode (inner lines) in 0.10 M KCl solution containing 5.0 mM $K_3Fe(CN)_6$ at a scan rate of 20 mV/s. Arrows indicate the redox waves likely due to oxides on the carbon nanotube surface, which contribute a "pseudocapacitive" faradaic current at the potential from −0.40 to 0.20 V.

the carbon nanotube surface. The air film can be removed by pretreating the electrode in 1.0 N HNO_3 for about 5 min and cycling the potential in aqueous electrolytes between −0.50 V and +1.20 V several times before obtaining the desired measurements. This procedure was found to be sufficient to activate the electrode and create a better electrolyte/electrode interface in aqueous solutions.

Results

SWNTP Electrode. As mentioned before, the large effective capacitance of the SWNTP electrode has been thoroughly investigated in simple supporting electrolytes such as 1.0 M NaCl, 1.0 M KOH, and 1.0 M H_2SO_4.[9] To understand the electron-transfer property of this electrode, $K_4Fe(CN)_6$ is introduced in the electrolyte as the redox benchmark in this study. Figure 1 shows CVs obtained with a SWNTP electrode and a CPE. These data are normalized to the geometric area of the electrode surface. Both sides of the SWNTP were taken into consideration. The CV obtained with the CPE shows the typical feature, i.e., a pair of redox waves centered at about 0.25 V superimposed on the small background current (attributed to the double-layer capacitance). GCE gives almost the same redox waves (not shown here) but the baseline separation is roughly doubled, indicating a larger effective surface area consistent with the literature.[5] The peak separation is about 96 mV for CPE and GCE, which is larger than $\sim$60 mV for the ideal reversible one-electron-transfer reaction, indicating quasi-reversible processes between the $Fe(CN)_6^{3-}/Fe(CN)_6^{4-}$ couple and the electrodes. It normally takes substantial pretreatment to approach $\sim$60 mV peak separation with these carbon electrodes.[5] With the SWNTP electrode, the peak height and the position of the redox waves are nearly the same as those with CPE and GCE. However, the background currents in forward and backward scans are now well separated. This agrees well with the large capacitance feature reported before.[8,9] Clearly, the CV of the SWNTP electrode, as expected, is the superposition of two contributions: (1) a large background current due to the capacitance, and (2) the quasi-reversible redox waves of the $K_3Fe(CN)_6/K_4Fe(CN)_6$ couple. They can be obtained in the same experiment and correlated to the structure of the electrode to give us better understanding.

To further understand these two contributions, we measured the CV at a series of scan rates ranging from 10 to 250 mV/s. The anodic current (I_a) and cathodic current (I_c) at potential

Novel Three-Dimensional Electrodes

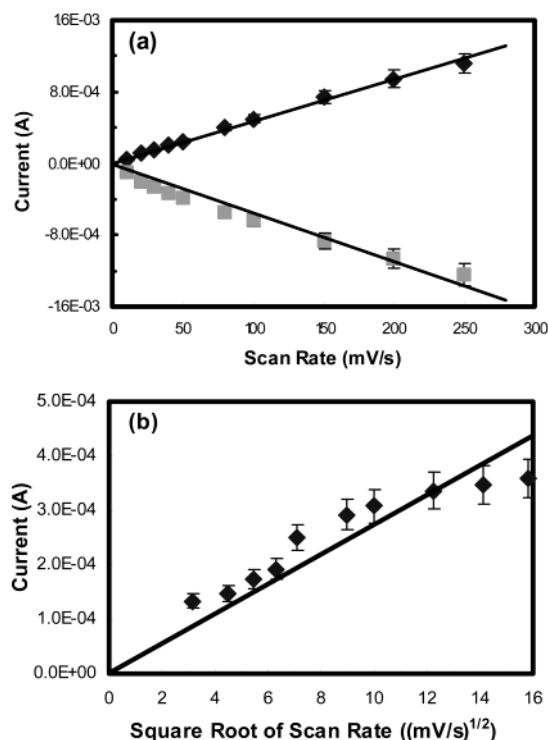*J. Phys. Chem. B, Vol. 106, No. 36, 2002* **9301**

Figure 2. (a) Anodic current (diamonds) and cathodic current (squares) of the cyclic voltammetry at −0.05 V (vs Ag/AgCl (3M KCl)) obtained with the SWNTP electrode vs the scan rate. (b) The fitted anodic peak height of the $Fe(CN)_6^{3-}/Fe(CN)_6^{4-}$ pair using SWNTP electrode vs the square root of the scan rate.

$E = -0.05$ V are selected to represent the baselines and plotted vs the scan rate (ν) in Figure 2a. Clearly, they are linearly proportional to the scan rate, indicating that the baseline current corresponds to the capacitive charge−discharge current. The current can be simply expressed as

$$I = C \cdot dE/dt \qquad (1)$$

where dE/dt is the linear scan rate ν in CV measurements. The capacitance could consist of two contributions: (1) the capacitance due to the double-layer at the electrode/electrolyte interface, which is proportional to the effective surface area, and (2) the "pseudocapacitance" due to the surface faradaic reaction of redox active oxides such as various quinones formed during acid treatment in the sample preparation.[5] The weak and broad oxidation wave around −0.05 V and the reduction wave around −0.20 V (indicated by the arrows in Figure 1) are likely due to the latter, similar to those observed by Barisci et al. in 1.0 M NaCl.[9] This might be the reason that the effective capacitance below 0.2 V is larger than that above 0.4 V. However, the pseudocapacitance only accounts for about one-third of the observed value of the effective capacitance. The double-layer capacitance is still the major component and can be used as a parameter to characterize the accessible surface area in these porous materials.

By taking the average baseline separation between the forward and backward scans, we can calculate the surface specific capacitance to be about 125 $\mu F/mm^2$, which is about 3 to 4 orders of magnitude higher than conventional carbon electrodes (varying from 0.02 to 0.2 $\mu F/mm^2$).[5] This is due to the fact that SWNTP is a highly permeable porous film. Electrolytes can penetrate through the film and gain access to the interior surface. Considering the thickness of the SWNTP (about 10 μm), we obtained a volume specific capacitance of 6.25 F/cm^3 and a

weight specific capacitance of about 16.9 F/g (calculated using the density of 0.37 g/cm^3). These values are in good agreement with the previous report.[9] It is worth noting that, at moderate scan rates (10 to 250 mV/s) in this study, there is sufficient time for the electrolyte to diffuse through the narrow pores; the so-called "slow capacitance"[5] is likely included in the baseline. Therefore, the whole exposed surface area contributes to the effective capacitance.

We also fit the peak heights for the anodic (I_{pa}) and cathodic (I_{pc}) waves. The cathodic wave is not resolved enough to give a good fit, so only the anodic peak height is plotted in Figure 2b. The I_{pa} was found to be a linear function of the square root of the scan rate at moderate scan rates (10 to 200 mV/s), which is similar to a solid macroelectrode rather than nanoelectrode ensembles.[6] This is likely because the SWNTP has a very high packing density with average pore sizes of tens of nm, much smaller than the diffusion layer thickness ($\sim \sqrt{Dt}$, normally over microns). The diffusion layers originating at individual CNTs and/or CNT bundles are heavily overlapped, resulting in the semiinfinite planar diffusion of bulk redox species similar to a solid planar macroelectrode. Only at high scan rates (over 200 mV/s) does the porous nature start to show effects. We observe that the data point at 250 mV/s deviates from the linear curve. It is noted that the capacitive background current increases much faster than the faradaic current as the scan rate is increased. With the huge effective capacitance of SWNTP, it is difficult to fit the precise peak height at scan rates above ∼200 mV/s. The peak separation also increases with the scan rate ($\Delta E_p = 168$ mV at 100 mV/s vs $\Delta E_p = 100$ mV at 20 mV/s), indicating a quasi-reversible process likely as the result of both the slow electron transfer at the CNT surface (due to graphite basal plane-like structure) and the slow diffusion through the narrow pores.

It is noteworth that the chemical and electrochemical properties of the SWNTs are strongly dependent on the post growth processing procedures. Liu[8] simply cast the SWNT film from SDS suspension and measured in acetonitrile solutions, while our study and Barisci's study[9] involve prolonged strong acid treatment as reported before.[15] While both methods can produce SWNT film with large capacitance, the latter one is more suitable for applications in aqueous solutions. The acid treatment likely creates more oxide defects on the side walls and makes the SWNT film more hydrophilic so that the aqueous solution can contact the surface better. As a result, the electron transfer rate can be improved. On the other hand, the acid preteatment also introduces extra redox waves at potentials less than 0.20 V, which likely corresponds to the reduction/oxidation of quinones. These reduction waves were not observed in Liu's study at the proper potentials (0 to −1.0 V vs Ag quasi-reference electrode), likely due to the absence of quinone-like oxides by the mild post growth processing conditions.

As-Produced MWNTT Electrode. It seems to be straightforward to repeat the above measurements with the MWNTs. However, it is difficult to prepare similar thin papers with MWNTs. MWNT samples tend to form powder instead of paperlike sheets. An alternative solution is to grow MWNT films directly on solid substrates with a conducting metal layer. Details of the sample preparation and characterization were published elsewhere.[16] TEM measurements showed that the multiwalled carbon nanotubes have clear hollow channels and highly ordered graphitic side walls.[16] The SEM image in Figure 3a shows the edge of such a film, indicating that nanotubes form a rather uniform film with the thickness variable from 30 to 100 μm. The high-resolution SEM image in Figure 3b shows that the
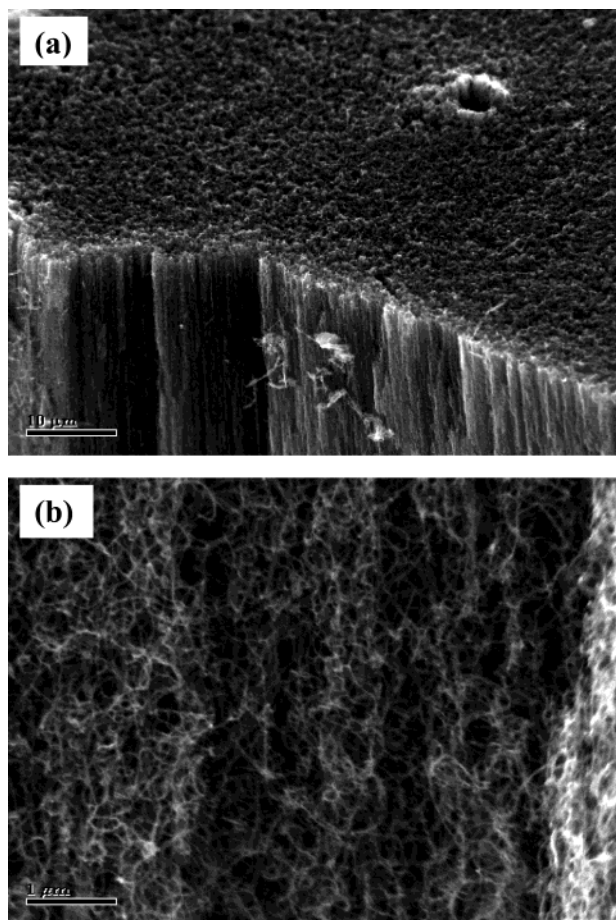
Figure 3. Scanning electron microscopy images with 45° perspective view (a) at the top corner and (b) at the side of an as-produced multiwalled carbon nanotube tower sample by thermal chemical vapor deposition. Scale bars are 10 μm and 1 μm, respectively.
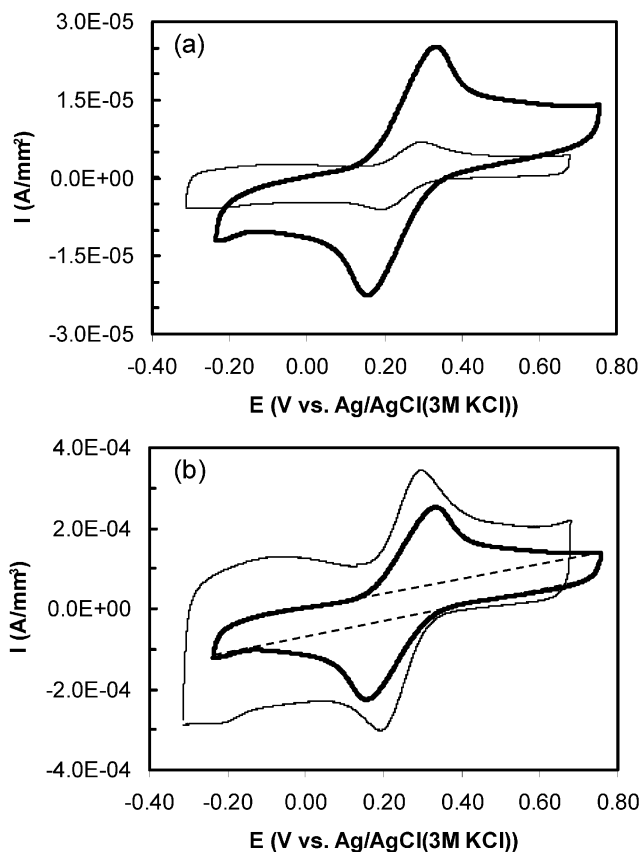

Figure 4. The cyclic voltammetry obtained with a multiwalled nanotube tower electrode (thick lines) in comparison to that with a single-walled nanotube paper electrode (thin lines) in 0.10 M KCl solution containing 5.0 mM $K_3Fe(CN)_6$ at a scan rate of 20 mV/s after (a) normalized to the geometric surface area, and (b) normalized to the geometric volume of the carbon nanotube films. The dashed lines indicate the capacitive background currents which are almost perfectly parallel to each other.

nanotubes are randomly curved in the submicron range but overall are aligned along the surface normal. Therefore, we refer to these samples as MWNT towers. The diameter of MWNTs varies from ~15 nm to 80 nm with the highest abundance around 35 nm.[16] The average nanotube separation is about 100 to 200 nm, a few times larger than that between SWNT bundles in the SWNTP. We expect that this electrode would give similar porous characteristics in CV as the SWNTP. However, to our surprise, they appear very different.

As shown in Figure 4a, the redox current normalized to the geometric surface area with the MWNT electrode is clearly much bigger than that of the SWNTP electrode. After careful examination, we realized that the thickness of the MWNTT samples (varying from 30 to 100 μm) is much larger than that of the SWNTP (about 10 μm). The CV measurements with a series of samples of different thickness indicate that the redox current is approximately proportional to the film thickness. Since the nanotube film is a highly porous material, electrolytes likely access the interior surface. As a result, the volume instead of the geometric area of the outer surface should be considered for the capacitance, which is quite different from a solid electrode.

Figure 4b shows the same CVs after normalization to the volume of the CNT film. The redox peak areas of the $Fe(CN)_6^{3-}$/$Fe(CN)_6^{4-}$ couple in these two samples are almost the same. However, the peak separation with MWNTT electrode is about 170 mV, much larger than the 100 mV separation with the SWNTP electrode. The effective capacitance is only about 2.0 F/cm^3, and the baselines are perfectly parallel and closer to each

other in the MWNTT electrode, behaving like an ideal double-layer capacitor. The weak redox waves at −0.05 V and −0.20 V observed with the SWNT paper electrode are not present with the MWNTT electrode. The integrated area under the oxidation wave is 2.1 × 10^{-3} C/mm^3 for the MWNTT electrode, almost the same as the value of 1.7 × 10^{-3} C/mm^3 for the SWNTP electrode, in contrast to the dramatic change in the capacitance.

Heat-Treated MWNTT Electrode. It is interesting that the volume-specific capacitance of the MWNTT electrode is much smaller than that of the SWNTP electrode. This could be due to three possibilities: (1) the as-produced MWNT surface is highly hydrophobic so that aqueous solutions cannot penetrate and access the CNT surface interior of the film, (2) there is some material on the CNT surface or between CNTs blocking the electrolyte solution, and (3) the pseudocapacitance is absent in this sample. To clarify these issues, we carried out CV measurements in 1.0 mM ferrocene dissolved in nonaqueous acetonitrile solution (Sigma-Aldrich) containing 0.10 M tetrabutylammonium perchlorate (Fluka). The CVs obtained from both of SWNTP and MWNTT electrodes are similar to those in aqueous solution, excluding the first possibility.

It is well known that there is a significant amount of amorphous carbon, graphitic particles, and catalyst particles mixed with the MWNTs during thermal CVD. Our TGA results showed that about 40 to 50% of the weight is lost after the sample is heated to 500 °C for a few hours in air.[17] Figure 5 shows an SEM image of the edge of a MWNTT sample after heat-treatment in air at 450 °C for 10 h. Compared to Figure

Novel Three-Dimensional Electrodes

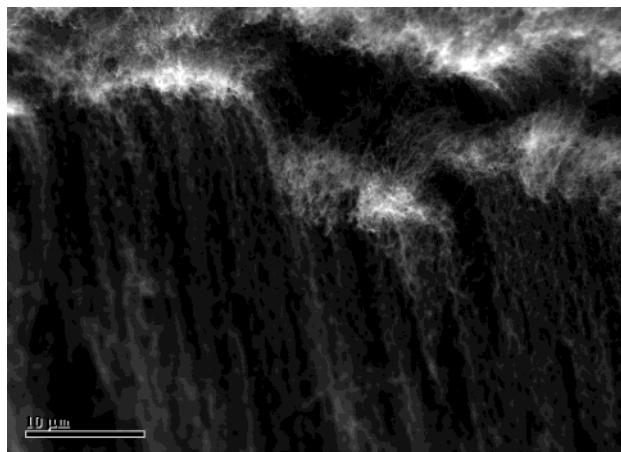*J. Phys. Chem. B, Vol. 106, No. 36, 2002* **9303**

Figure 5. Scanning electron microscopy image with 45° perspective view at at the top corner of the multiwalled nanotube tower sample after heat treatment in air at 450 °C for 10 h. The scale bar is 10 μm.
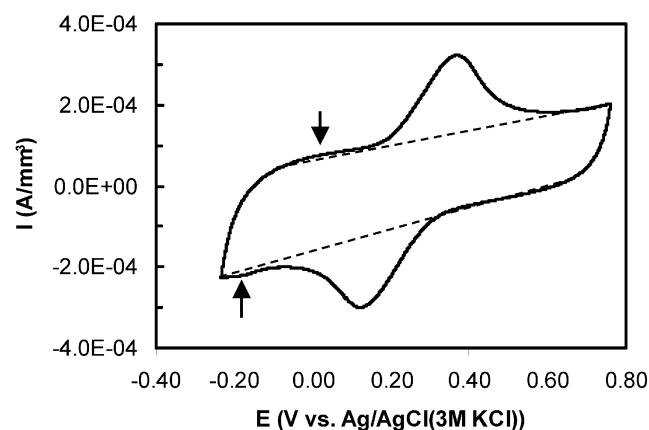

Figure 7. Scanning electron microscopy image of top view of a heat-treated multiwalled carbon nanotube tower electrode after removing from the solution and slowly drying in air. The scale bar is 10 μm.

Figure 6. Cyclic voltammetry obtained with a heat-treated multiwalled nanotube tower electrode in 0.10 M KCl solution containing 5.0 mM $K_3Fe(CN)_6$ at a scan rate of 20 mV/s. Arrows indicate a pair of redox waves likely due to surface oxides on the nanotubes. The dashed lines indicate the baselines of the capacitive current. The separation at low potential is clearly larger due to the "pseudocapacitive" faradaic reaction of the surface bonded oxides.

3a, it is much more fluffy. The heat treatment likely removed most of the amorphous carbon, which previously randomly filled between the CNTs or coated individual CNTs but was not directly observed by SEM. The thermally more stable MWNTs seem to survive the heat treatment procedure. As a result, the heat-treatment creates a more opened porous structure in which a larger CNT surface is accessible by electrolytes.

Figure 6 shows the CV obtained with the heat-treated MWNTT sample. Compared to the as-produced sample, the capacitance is dramatically increased. Interestingly, the shape of the CV becomes asymmetric with a larger separation in the negative potential region similar to SWNTP electrodes. The weak redox waves between −0.30 and 0.0 V also appear. The volume-specific capacitance is about 4.7 F/cm^3, more than double that of the as-produced MWNTT sample (2.0 F/cm^3), but still much smaller than that of the SWNTP electrode (6.25 F/cm^3). The peak separation is increased to about 230 mV. It is likely that the mild heat-treatment removes most amorphous carbon and exposes more side walls of the MWNTs. Since the side wall of the CNT is similar to the graphite basal plane, a very slow electron transfer rate is expected. This might be the reason that the as-produced MWNTTs has larger peak separation than the extensive acid-treated SWNTP electrode, which presents high-density edge-plane like defects. Similar to the acid
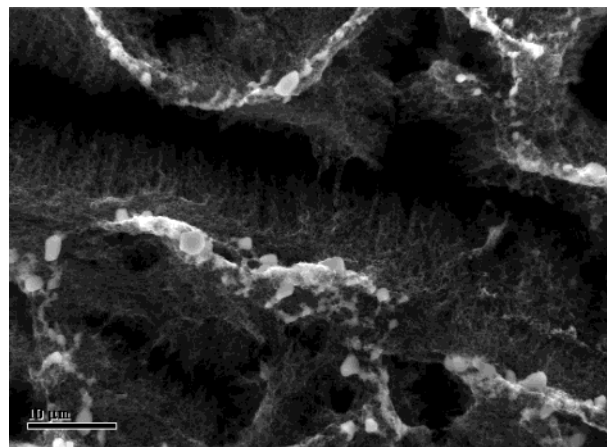
treatment, the heat treatment induces oxidation at the carbon nanotube surface, but the density of these sites is much lower than that in the prolonged acid-treated SWNTP. The volume normalized anodic peak area is 1.8×10^{-3} C/mm^3, about the same as the SWNTP (1.7 C/mm^3) and MWNTT electrodes (2.1 C/mm^3), which further supports that the volume instead of the outer surface of the film needs to be considered.

Interestingly, after we took the heat-treated MWNTT electrode out from the solution and let it dry slowly in air, the nanotube film gradually curled and peeled off from the Si substrate. An SEM image in Figure 7 shows that the fluffy heat-treated nanotube film collapses into strips of dense bundles. The width of the strip is over 10 microns and the length is extended over hundreds of microns. Relatively large open space is left between the strips. In contrast, the as-produced MWNTT sample did not show this phenomenon. This is another piece of evidence indicating that the heat treatment opens up more space in the CNT film. During the drying process, the strong capillary force of water droplets pulled nanotubes together to form dense bundles. The as-produced sample has a large amount of amorphous carbon to glue nanotubes into bundles, which blocks out the solution as well as increases the mechanical stability, resulting in a less porous electrode compared to the heat-treated samples. This agrees well with the capacitance change obtained by electrochemical measurements.

Discussion

For a nanoelectrode ensemble, the density/separation of individual electrodes is critical.[6] As observed with the densely packed SWNTP electrodes, the diffusion layers of individual CNT likely overlap. As a result, the CV of this kind of electrodes in measuring the redox species in bulk solution is similar to a solid planar macroelectrode. For less dense, i.e., more porous, MWNTT electrodes, the CV is in a different regime. It is interesting to note that, for all three CNT samples, the integrated anodic peak area is about the same (considering the experimental errors) if normalized to the geometric volume instead of the geometric surface area of the CNT film. For the 30−100 μm thick MWNTTs that we used, we realized that there is certain amount of redox species present within the volume of the electrode. It can be calculated that about 5×10^{-9} mol/mm^3 $K_4Fe(CN)_6$ is present within the porous electrode accounting for a total charge of about 4.82×10^{-4} C/mm^3 in the oxidation wave. This is smaller than the average value of 1.9×10^{-3} C/mm^3 under the anodic wave with all three kinds of CNT

9304 *J. Phys. Chem. B, Vol. 106, No. 36, 2002*

Li et al.

ensembles. One can speculate that, in addition to the redox species in the solution trapped in this volume, the huge surface area cannot be neglected. Surface adsorption also likely increases the amount of $K_4Fe(CN)_6$ molecules within the CNT electrode ensembles. The CNT electrode ensemble is obviously a 3-D structure with a faradaic current in the CV contributed from all three processes: (1) the redox species diffused from bulk solution to the ensemble, (2) the redox species adsorbed on the interior CNT surface of the whole ensemble, and (3) the redox species in solution present in the open volume of the ensemble. Further modeling or experiments with a series of MWNTT electrodes with different thickness and density as well as different pretreatments are needed to understand the 3-D ensemble electrodes. In general, the CVs of these CNT ensembles are quite different from other permeable porous carbon electrodes such as carbon paste and graphite rods.[5]

In a previous report using a single MWNT bundle electrode,[13] fast electron transfer was observed with $K_3Fe(CN)_6/K_4Fe(CN)_6$, couple even though the electrode was not subjected to any pretreatment. An ideal Nernstian behavior with about 60 mV peak separation was observed. MWNT paste packed in the glass tube also showed fast electron transfer for dopamine oxidation[18] and oxygen reduction.[19] However, this is not the case for all three CNT electrodes used in our study. The large peak separation ($>$100 mV) indicates a quasi-reversible slow electron transfer process. This is likely due to the fact that the open end of CNTs, which can give fast electron transfer (similar to edge-plane of graphite[5]), is only a very small portion of the CNT surface exposed to electrolytes in our samples. Side walls and an amorphous carbon-covered surface dominate most of the surface. Similar to other carbon materials, pretreatment is important in improving the electron transfer rate. The extensive acid treated SWNTP has shown the smallest ΔE_p among the three types of electrodes. Because ΔE_p is in the decreasing order for SWNTP $<$ MWNTT $<$ heat-treated MWNTT, completely reversing that of CNT packing density, we can exclude the possibility that the slow diffusion through the narrow pore in the ensemble dominates the observed electron transfer rate. The electrochemical properties of CNTs seem to be dominated by the graphite basal plane nature. The CNT growth conditions might be also important. The MWNTs with fast electron transfer rates were prepared with an electric arc discharge process[13] at temperatures much higher (over 2000 °C) than our thermal CVD process (at ~750 °C). This may result in quite different graphitic structures in the grown CNTs.

For different applications, the faradaic redox current and the capacitive background can be optimized by changing the CNT density. For example, applications in energy storage media or supercapacitors require dense SWNTP due to its highest volume specific capacitance. On the other hand, the electrochemical sensor application requires the best signal (mainly from faradaic current due to redox species) to background (mainly due to the capacitive charge/discharge) ratio. Therefore, the density of CNTs needs to be reduced so that the intertube distance is in the same order of magnitude as the diffusion layer thickness. The high sensitivity neurotransmitter sensor demonstrated recently by Ng et al.[20] was attributed to the reduced density controlled by the soft-lithographic method. We have recently fabricated 2-D CNT nanoelectrode ensembles using vertically aligned MWCNTs followed by dielectric filling to insulate the side walls.[21] The exposed MWCNT ends should behave like a graphite edge-plane, resulting in a nanoelectrode ensemble for electroanalytical applications requiring fast electron transfer rates.
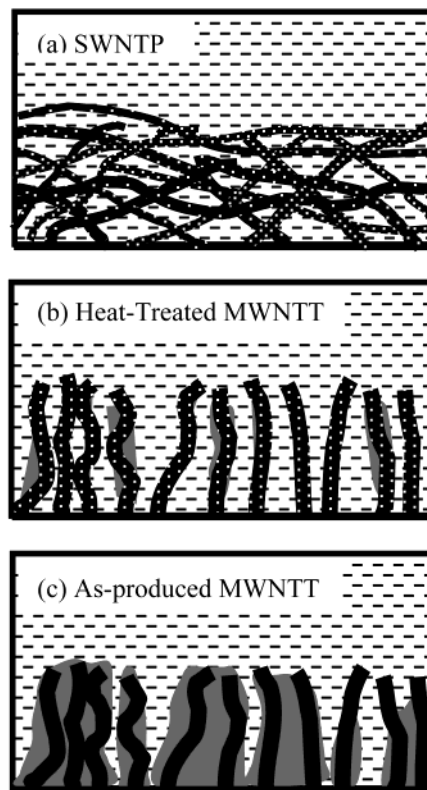

Figure 8. Schematic of the three CNT ensemble electrodes presented in the order of the effective capacitance. The white dots on the CNTs represent defects created by pretreatments to give graphite edge-plane electrochemical properties. Gray color represents amorphous carbon around the CNTs.

Conclusions

As summarized in Figure 8, we present the electrochemical characterization of three different carbon nanotube ensemble electrodes: SWNTP, as-produced MWNTT, and heat-treated MWNTT. The electrochemical results reveal two types of information: the capacitive current and the faradaic current due to the redox reaction of $K_3Fe(CN)_6/K_4Fe(CN)_6$ pairs presented in the solution as a benchmark. The capacitance indicates the change in total surface area as well as the density of surface oxides. For these 3-D ensembles, the total surface area includes both the surface of CNTs interior of the film and that at the outer surface of the film. The value of the effective capacitance is in the following order: as-produced MWNTT $<$ heat-treated MWNTT $<$ SWNTP. SWNTP has the largest effective capacitance due to its highly dense packing while the film still remains permeable by electrolytes. We have found that a large portion of the CNT surface of the as-produced MWNTT electrode is blocked by impurities mainly consisting of amorphous carbon. These materials can be largely removed by prolonged heat treatment at 450 °C in air as indicated by the increase in the capacitance. The SEM image and the collapsing phenomena after removing the sample from aqueous solution further confirm that the heat treatment opens up more space in the interior of the film. The electron transfer rate indicated by ΔE_p of the $K_3Fe(CN)_6/K_4Fe(CN)_6$ pairs decreases in a different order: SWNTP $>$ as-produced MWNTT $>$ heat-treated MWNTT. This is related to the extent of side-wall exposure and the density of graphite edge-plane-like defects created in pretreatments. The redox reaction of $K_3Fe(CN)_6/K_4Fe(CN)_6$ is found to occur not only at the outer surface of the CNT film but also interior of the film. Both faradaic redox current and the capacitive background need to be normalized to the geometric volume

Novel Three-Dimensional Electrodes

J. Phys. Chem. B, Vol. 106, No. 36, 2002 **9305**

instead of the geometric surface area of the CNT film. This indicates that the CNT ensemble behaves as a 3-D electrode. Since all the redox species inside the film as well as those diffusing from the bulk solution can be measured, the faradaic signal can be significantly enhanced compared to a solid electrode. The signal or background can be optimized by controlling the CNT packing density, i.e., intertube distance, depending on the application needs.

References and Notes

(1) Dresselhaus, M. S.; Dresselhaus, G.; Eklund, P. C. *Science of Fullerenes and Carbon Nanotubes*; Academic Press: New York, 1996.

(2) Ebbessen, T. W. *Carbon Nanotubes: Preparation and Properties*; CRC Press: Boca Raton, FL, 1997.

(3) Saito, R.; Dresselhaus, M. S.; Dresselhaus, G. *Physical Properties of Carbon Nanotubes*; Imperial College Press: London, 1998.

(4) Tománek, D.; Enbody, R. *Science and Application of Nanotubes*; Kluwer Academic: New York, 2000.

(5) McCreery R. L. In *Electroanalytical Chemistry*; Bard, A. J., Ed.; Marcel Dekker: New York, 1991; vol. 17, pp 221−374.

(6) Menon, V. P.; Martin, C. R. *Anal. Chem.* **1995**, *67*, 1920.

(7) Xie, Q.; Arias, F.; Echegoyen, L. *J. Am. Chem. Soc.* **1993**, *115*, 9818.

(8) Liu, C.-Y.; Bard, A. J.; Wudl, F.; Weitz, I.; Heath, J. R. *Electrochem. Solid-State Lett.* **1999**, *2*(11), 577.

(9) Barisci, J. N.; Wallace, G. G.; Baughman, R. H. *J. Electrochem. Soc.*, **2000**, *147*(12), 4580.

(10) Bachtold, A.; Henny, M.; Terrier, C.; Strunk, C.; Schönenberger, C.; Salvetat, J.-P.; Bonard, J.-M.; Forró, L. *App. Phys. Lett.* **1998**, *73*(2), 274.

(11) Chen, J. H.; Li, W. Z.; Huang, Z. P.; Wang, D. Z.; Yang, S. X.; Wen, J. G.; Ren, Z. F. Proceedings of the 197th Meeting of the Electrochemical Society; Electrochemical Society: Pennington, NJ, 2000.

(12) Campbell, J. K.; Sun, L.; Crooks, R. M. *J. Am. Chem. Soc.* **1999**, *121*, 3779.

(13) Nugent, J. M.; Santhanam, K. S. V.; Rubio, A.; Ajayan, P. M. *Nano Lett.* **2001**, *1*(2), 87.

(14) Thess, A.; Lee, R.; Nikolaev, Pl; Dai, H.; Petit, P.; Robert, J.; Xu, C. H.; Lee, Y. H.; Kim, S. G.; Rinzler, A. G. Colbert, D. T.; Scuseria, G. E.; Fischer, J. E.; Smalley, R. E. *Science* **1996**, *273*, 483.

(15) Liu, J.; Rinzler, A. G.; Dai, H.; Hafner, J. H.; Bradley, R. K.; Boul, P. J.; Lu, A.; Inverson, T.; Shelimov, K.; Huffman, C. B.; Rodriguez-Macias, F.; Shon, Y.-S.; Lee, T. R.; Colbert, D. T.; Smalley, R. E. *Science* **1998**, *280*, 1253.

(16) Delzeit, L.; Nguyen, C. V.; Chen, B.; Stevens, R.; Cassell, A.; Han, J.; Meyyappan, M. *J. Phys. Chem. B* **2002**, 106, 5629.

(17) Li, J.; Nguyen, C. V.; Chen, B.; Delzeit, L.; Cassell, A.; Han, J.; Meyyappan, M., to be published.

(18) Britto, P. J.; Santhanam, K. S. V.; Ajayan, P. M. *Bioelectrochem. Bioenerg.* **1996**, *41*, 121.

(19) Britto, P. J.; Santhanam, K. S. V.; Rubio A.; Alonso, A.; Ajayan, P. M. *Adv. Mater.* **1999**, *11*(2), 154.

(20) Ng, H. T.; Fang, A. P.; Li, J.; Li, S. F. Y. *J. Nanosci. Nanotech.* **2001**, *1*(4), 375.

(21) Li, J.; Stevens, R.; Delzeit, L.; Ng, H. T.; Cassell, A.; Han, J.; Meyyappan, M. *App. Phys. Lett.* **2002**, *81*(5), 910.